Journal of Visualized Experiments

A combined approach using structural DNA alteration analysis in conjunction with patient-derived xenografts to test targeted therapies in cancer

--Manuscript Draft--

Article Type:	Invited Methods Article - JoVE Produced Video
Manuscript Number:	JoVE59362R2
Full Title:	A combined approach using structural DNA alteration analysis in conjunction with patient-derived xenografts to test targeted therapies in cancer
Keywords:	Genomic analysis, Mate-pair sequencing, Patient derived xenografts, DNA alteration validation, Targeted therapy
Corresponding Author:	Irina V Kovtun, Ph.D. Mayo Clinic Minnesota Rochester, MN UNITED STATES
Corresponding Author's Institution:	Mayo Clinic Minnesota
Corresponding Author E-Mail:	ivkru@yahoo.com
Order of Authors:	Irina V Kovtun, Ph.D.
	Lin Yang
	Faye R. Harris
	Piyan Zhang
	George Vasmatzis
Additional Information:	
Question	**Response**
Please indicate whether this article will be Standard Access or Open Access.	Standard Access (US$2,400)
Please indicate the **city, state/province, and country** where this article will be **filmed**. Please do not use abbreviations.	Rochester, MN, usa

TITLE:

Using Structural DNA Alteration Analysis in Conjunction with Patient-Derived Xenografts to Test Targeted Cancer Therapies

AUTHORS AND AFFILIATIONS:

Lin Yang[1], Faye R. Harris[1], Piyan Zhang[1], George Vasmatzis[1,2], Irina V. Kovtun[1,3]

[1]Center for Individualized Medicine, Mayo Clinic, Rochester, MN, USA
[2]Molecular Medicine, Mayo Clinic, Rochester, MN, USA
[3]Molecular Pharmacology and Experimental Therapeutics, Mayo Clinic, Rochester, MN, USA

Corresponding Author:

Irina V. Kovtun (ivkru@yahoo.com)

KEYWORDS:

genomic analysis, mate-pair sequencing, patient derived xenografts, tumor engraftment, DNA alteration validation, targeted therapy

SUMMARY:

Presented here is a protocol to test the efficacy of targeted therapies that are selected based on the genomic makeup of tumors. The protocol describes identification and validation of structural DNA rearrangements, engraftment of patient tumors into mice, and testing of responses to corresponding drugs.

ABSTRACT:

The combination of next-generation sequencing technologies, subsequent analyses, validation of therapeutic targets, and testing of sensitivity for drugs in patient-derived xenografts (PDX) is a promising approach to aid treatment decisions in cancer patients. Presented in this protocol is proof-of-principal for this strategy, using ovarian tumors for genomic analyses and treatment testing as an example. The mate-pair next-generation sequencing (MPseq) protocol is used to identify chromosomal rearrangements, including gene fusions and copy number changes, in primary tumors. Further analysis is then performed to determine alterations that may be therapeutically targeted. Selected genomic alterations are validated with individualized primers for DNA chromosomal rearrangements in the tumor DNA (original and derived from PDX). The tumor is grown in immunocompromised mice until palpable, and treatments are administered with drugs that are selected based on genomic analyses. Results demonstrate a good correlation between the predicted and observed responses in the PDX model. This approach can be used to test the efficacy of combination treatments that include targeted drugs.

INTRODUCTION:

Patient-derived xenografts (PDXs), which are generated from the implantation of patient tumor samples into immunodeficient mice, have emerged as a powerful preclinical model to aid personalized anti-cancer care. PDX models have been successfully developed for a variety of human malignancies. These include breast and ovarian cancers, malignant melanoma,

colorectal cancer, pancreatic adenocarcinoma, and non-small cell lung cancer[1-5]. Tumor tissue can be implanted orthotopically or heterotopically. The former, considered more accurate but technically difficult, involves transplantation directly into the organ of tumor origin. These types of models are believed to precisely mimic histology of the original tumor due to the "natural" microenvironment for the tumor[6,7]. For example, orthotopic transplantation into the bursa of the mouse ovary has resulted in tumor dissemination into the peritoneal cavity and the production of ascites, typical of ovarian cancer[8]. Similarly, injection of breast tumors into the thoracic instead of abdominal mammary gland has been shown to affect PDX success rate and behavior[9]. However, orthotopic models require sophisticated imaging systems to monitor tumor growth. Heterotopic implantation of solid tumor is typically performed by implanting tissue into the subcutaneous flank of a mouse, which allows easier monitoring of tumor growth and is less expensive and time-consuming[7]. However, tumors grown subcutaneously have been shown to rarely metastasize, unlike those observed in cases of orthotopic implantation[10].

The success rate of engraftment has been shown to vary and greatly depends on tumor type. More aggressive tumors and tissue specimens containing higher percentages of tumor cells have been reported to show better success rates[12,13]. Consistent with this, tumors derived from metastatic sites have been shown to engraft at frequencies of 50%–80%, while those from primary sites have engrafted at frequencies as low as 14%[12]. In contrast, tissue containing necrotic cells and fewer viable tumor cells engraft poorly. Tumor growth can also be promoted by the addition of basement membrane matrix proteins into the tissue mix at the time of the injection into mice without compromising properties of the original tumor[14]. The size and number of tissue pieces intended for implantation have also been found to affect the success rate of engraftment. Greater tumor take-rates have been reported for implantation in the sub-renal capsule compared to subcutaneous implantation due to the sub-renal capsule's ability to maintain original tumor stroma and provide the host with stromal cells, as well[15].

Most studies use NOD/SCID immunodeficient mice, which lack natural killer cells[16], and have been shown to increase tumor engraftment, growth, and metastasis compared to other strains[14]. However, additional monitoring is required, as they may develop thymic lymphomas as early as at 3–4 months of age[13]. In ovarian tumor transplants grown in SCID mice, the outgrowth of B cells has been successfully inhibited by rituximab, preventing the development of lymphomas without impacting the engraftment of ovarian tumors[17].

More recently, NSG (NOD.Cg-*Prkdc*^{scid} *Il2rg*^{tm1Wjl}/SzJ) mice, carrying a null mutation in the gene encoding the interleukin 2 receptor gamma chain[18], has become a frequently used strain for the generation of PDX models. Tumors from established PDX models passaged to future generations of mice are reported to retain histological and molecular properties for three to six generations[19,20]. Numerous studies have shown that treatment outcomes in PDX models mimic those of the corresponding patients[2-4,21-23]. The response rates to chemotherapy in PDX moles for non-small lung cancer and colorectal carcinomas have been shown to be similar to those in clinical trials for the same drugs[24,25]. In co-clinical trials, PDX models developed for patients enrolled in clinical trials have been treated with the same drugs and have demonstrated parallel clinical responses in patients[2-4].

Coupling PDX models with high-throughput genomic analyses of tumors further strengthens the power of the PDX platform to study correlations between specific genomic alterations and therapeutic response. A number of studies have reported reproducibility and clinical translatability of this approach[26,27]. Testing the efficacy of the EGFR inhibitor cetuximab in a set of colorectal PDX models, Bertotti et al. found a correlation between the therapeutic effect and presence of EGFR amplification[28]. The responses observed in PDX models were consistent with the clinical responses to cetuximab in patients.

There are a few challenges associated with the development and application of PDX models. Among those is tumor heterogeneity[29,30], which may compromise the accuracy of treatment response interpretation, as a single cell clone with higher proliferative capacity within a PDX can outgrow the other ones[31] and result in loss of heterogeneity. Additionally, when single tumor biopsies are used to develop PDXs, some cell populations may be missed and are not represented in the final graft. Multiple samples from the same tumor are recommended for implantation to resolve this issue. Although PDX tumors tend to contain all cell types of the original donor tumor, these cells are gradually substituted by those of murine origin[3]. Functional crosstalk between murine stroma and human tumor cells is not fully understood. Co-injection of human tumor cells with patient-derived stromal cells has been shown to restore parts of the human tumor microenvironment in breast cancer PDXs[33].

Despite these limitations, PDX models remain among the most valuable tools for translational research as well as personalized medicine for selection of patient therapies. Major applications of PDXs include biomarker discovery and drug testing. PDX models are also successfully used to study drug resistance mechanisms and identify strategies to overcome drug resistance[34,35]. The approach described in the present manuscript allows identification of potential therapeutic targets in human tumors and assessment of the efficacy of corresponding drugs *in vivo* in mice harboring engrafted tumors that are initially genomically characterized. The protocol uses ovarian tumors engrafted intraperitoneally but is applicable to any type of tumor sufficiently aggressive to grow in mice.

PROTOCOL:

Fresh tissues from consenting patients with ovarian cancer were collected at the time of debulking surgery according to a protocol approved by the Mayo Clinic Institutional Review Board (IRB). All animal procedures and treatments used in this protocol were approved by the Mayo Clinic Institutional Animal Care and Use Committee (IACUC).

1. Mate pair sequencing and analyses

NOTE: Either fresh or flash frozen tissue must be used for mate-pair (MPseq) sequencing. Paraffin embedded material is not suitable because it contains fragmented DNA.

1.1. Isolate DNA from frozen tumor tissue. Use original human specimens obtained from surgical material or biopsy.

1.2. Use 1000 ng of DNA to make MPseq libraries and sequence as two samples per lane of HiSeq 2500 (see **Table of Materials**).

1.3. Analyze the data using a set of algorithms to detect large chromosomal aberrations (deletions, insertions, amplifications, inversions, and translocations) as described earlier[36,37].

2. Selection of therapeutic targets

2.1. Use the Panda tool (Pathway and Annotation) or an analogous tool to identify targetable alterations <http://bioinformaticstools.mayo.edu/Panda/>.

2.1.1. Make a list of genes that are identified as altered by MSeq as a simple tab-delimited file using standard accepted gene symbols.

2.1.2. Add a **#** sign to the header line of the list to ensure that the table header is transferred to the pathway level view of the software.

2.1.3. Upload the file by clicking the **Upload Annotation Set** navigation tab.

2.1.4. Assign a single icon from the menu to represent the underlying data by clicking on the icon of choice and then clicking the **Finalize** tab.

2.1.5. Review the page once the annotation files are uploaded to identify a column that displays the number of annotated genes per pathway per annotation. This is the last column on the right.

2.1.6. Use a **Pathway Filter** on the upper left of the main window to restrict the number of pathways displayed to the ones including genes of interest.

2.1.7. Identify pathways that have more genes annotated than expected by chance, using the function located under the **Enrichment** tab.

2.1.8. Select a database to display potentially druggable genes from **Preset Annotation** by checking an appropriate icon on the left of the main window (e.g., DGIdb, PharmGKB).

2.1.9. Select the pathway for visualization by clicking on its name displayed in the **Pathway Viewer** page.

NOTE: Icons representing each annotation set are displayed by next to the associated gene. Clicking on any gene in the pathway will open the corresponding GeneCards webpage in a new tab.

2.1.10. Select the pathways that show annotated genes of interest (i.e., altered in a given tumor) and "hits" for potential drugs for further analysis.

2.2. Use a database containing drugs approved for clinical application such as <https://clinicaltrials.gov/> to cross-reference the identified targets.

2.3. Prioritize targetable alterations for further testing in PDX models by performing a literature review (e.g., PubMed) to confirm relevance to the biology of a particular type of tumor.

3. Validation of genomic rearrangements by PCR and Sanger sequencing

3.1. Design primers using sequencing reads obtained from MPseq data.

3.1.1 Select a junction of interest for validation (i.e., potential therapeutic target) based on MPseq analyses.

3.1.2 Design primers directionally such that the amplicon contains the junction. Design two primers on each side of the junction, for a total of four, to increase the chances of amplifying the junction.

NOTE: Name primers as Case-Chromosome of region primer is written on-junction partner chromosome region-primer direction from case point of view (in cases of chromosomal inversions; the directions in the patient will be in opposite orientation to the reference genome).

3.1.3 Use standard PCR parameters for primer design and software such as Primer3. Select a melting temperature of 60–62 °C and GC content of 40%–60%. Make sure that predicted primer dimers, palindromes, or hairpin loops are absent.

3.1.4 Confirm that the primer lacks homology to other areas of the human genome using BLAT <http://genome.ucsc.edu/cgi-bin/hgBlat?command=start>.

3.2. Run a PCR to amplify the junction of interest.

3.2.1 Dilute primers to 10 mM and combine 10 µL of each primer so that each forward primer is paired with each reverse primer into a primer mix.

NOTE: Sequences for the primers for the selected example are shown in **Table 1**.

3.2.2 Label 0.2 mL strip tubes as: C1, T1, C2, T2, C3, T3, C4, and T4; where C = control pooled genomic DNA, T = tumor DNA, and the number indicates the primer mix.

3.2.3 Add 1 µL of each primer mix into the appropriately labeled tubes.

3.2.4 Prepare the Taq master mix by combining the reagents listed in **Table 2**, leaving the enzyme in the freezer until needed and adding it to the mix at the very end.

3.2.5 Create 2 master mixes, one for each template DNA,-control pooled genomic DNA and tumor DNA. Add 24 µL of each Taq master mix to its respective strip tube. The total reaction volume is 25 µL. Vortex very briefly, then spin the strip tube down.

3.2.6 Run a PCR in a thermocycler.

NOTE: Use the parameters shown in **Table 3**. Adjust the annealing temperature so it is at least 1 degree colder than the melting temperature of the primers. Store the completed PCR product at -20 °C (long-term) or refrigerated at 4 °C (short-term) until needed.

3.2.7 Perform electrophoresis to visualize PCR product using a 1.5% agarose gel. Leave a 2 µL aliquot of the product to be used for Sanger sequencing.

3.3. Perform Sanger sequencing to confirm the junction and identify the exact breakpoint.

3.3.1 Use the PCR product if the PCR generated a single product (band). Alternatively, cut the band out of gel, purify, and submit for Sanger sequencing along with the primer used for amplification.

4. Tumor engraftment and maintenance

4.1. Set up the preparations to engraft tumors into PDX mouse models.

4.1.1. Make sure that a supportive infrastructure is in place at the time of the start of development of any PDX models, including dedicated laboratory and animal facilities, skilled technical staff, and detailed standard operating procedures.

4.1.2. Ensure the quick transportation and processing of specimens, as speed is crucial for cell viability and successful engraftment.

4.1.3. Use a sterile environment to reduce bacterial and fungal contamination for processing and engrafting specimens.

4.1.4. Handle human specimens with caution and in accordance with institutional policies regarding potentially biohazardous materials, as they may harbor blood-borne pathogens.

4.2. Prepare the tissue for engraftment by putting the surgical specimen into a pre-chilled 50 mL tube with tissue culture media such as RPMI 1640.

4.2.1. Quickly transport the tissue to the laboratory to limit ischemia time to less than 30 min.

4.2.2. Confirm tumor content in the specimen by consulting a pathologist.

4.2.3. Place the tumor tissue in a dish containing cold PBS or in tissue culture media such as RPMI 1640 or DMEM containing antibiotics.

4.2.4. Identify and isolate viable tumor material from adjacent normal and necrotic tissue with help from a pathologist. Use sterile forceps and a scalpel to remove necrotic material identified by a pathologist.

NOTE: The tumor can be implanted either intraperitoneally or subcutaneously into the mice. Follow step 4.3 to perform intraperitoneal implantation, or skip to step 4.4 to perform subcutaneous engraftment. In this study, targeted therapies selected based on genomic analyses are tested in a series of PDX models for high grade serous ovarian cancer with intraperitoneal implantation.

4.3. To prepare the tissue for intraperitoneal implantation, mince the tissue with sterile forceps and a scalpel on ice to yield pieces approximately 0.3-0.5 cm^3 in size.

4.3.1. Mix the pieces 1:1 with ice-cold McCoy's media and inject 100 µL intraperitoneally into at least three female SCID mice.

4.4. To perform subcutaneous engraftment, cut the tumor tissue with sterile forceps, a scalpel, or surgical scissors into small fragments, roughly 2 mm x 2 mm x 2 mm in size, and transfer the fragmented tissues to a pre-chilled Petri dish on ice.

4.4.1. Add cold Matrigel to the dish with the fragmented tissue (approximately 200 µL per 10 pieces of tissue), mix well, and let the tissue fragments soak in the Matrigel for 10 min.

4.4.2. Anesthetize five female NOD/SCID mice to prepare for engraftment.

4.4.2.1. Place a mouse in a chamber containing isoflurane until it is fully anesthetized, using a chamber connected to precision vaporizer.

4.4.2.2. Confirm that the mouse is properly anesthetized by pinching the tail tip with atraumatic forceps.

4.4.2.3. Gently remove the fully anesthetized mouse from the chamber and put on a nose cone that has input from a vaporizer and output to a waste gas scavenging system.

4.4.3. Put vet ointment on the eyes to prevent dryness while under anesthesia.

4.4.4. Prepare the area where the surgery will be performed. Use aseptic techniques to perform the surgery.

4.4.4.1. Ensure that the surface of the surgical area is non-porous, sealed, and disinfected prior to surgery.

4.4.4.2. Begin the surgery with sterile (by autoclave, gas, or chemical sterilization) instruments.

4.4.4.3. Use gloves to handle the instruments and maintain sterility of the instrument tips throughout the procedure through submersion in ethanol between surgery steps.

4.4.5. Use sterile surgical scissors and forceps to create a 5–10 mm vertical skin incision on both flanks of a mouse.

4.4.6. Insert straight forceps gently into the subcutaneous space to create a pocket large enough for a tumor fragment to be placed under the fat pad.

4.4.6. Use the sterile straight forceps to insert tumor fragments into a previously prepared pocket in each of the five mice.

4.4.8. Close the skin incisions using tissue glue.

4.5. Intraperitoneally inject each mouse with 100 µL of rituximab after implantation to inhibit lymphocyte proliferation.

4.6. Place the mouse into a cage under a heat lamp for approximately 20 min until recovery from anesthesia. Monitor its vital signs and ensure sufficient hydration.

4.7. Return the mouse to the location of the other mice after recovery from anesthesia and give access to food and water.

4.8. Provide postoperative care and monitoring according to institutional guidelines. Check for signs of pain and distress daily for 3 consecutive days after surgery.

NOTE: Criteria for pain or distress include necrosis or ulceration, weight loss/body condition scoring, behavioral signs such as activity level, motor function, and posture.

4.9. Routinely check the mice for tumor formation bi-weekly until tumors reach a size of 0.5 cm in diameter, as measured by a caliper.

4.10. Assess the health score of each mouse as derived from appearance, behavior, and body condition[38]. Use scores of ≤6 as criteria for moribund mice to be sacrificed by carbon dioxide inhalation.

5. Testing responses to genomically identified targets in PDX models

5.1. Start the selected targeted treatments when the tumors are palpable and reach a size of 0.5 cm^3 as measured by an ultrasound scan.

5.1.1. Prior to performing an ultrasound scan of the abdomen, remove the mouse abdominal fur and apply a sterile jelly lubricant.

5.1.2. Use an ultrasound machine with a transducer to obtain images with the tumor positioned in cross-section. Obtain three measurements per session for each animal and average the value for a more accurate assessment of tumor size.

5.1.3. Analyze the images using available software[39].

5.2 Administer chemotherapy consisting of a mixture of carboplatin at 51 mg/kg and paclitaxel at 15 mg/kg intraperitoneally (IP) once a week for a total treatment duration of 4–6 weeks. Make sure that total volume for injection does not exceed 0.2 mL.

5.3. Make a MK-2206 stock solution in 30% Captisol and deliver via oral gavage at 120 mg/kg daily for 4 consecutive weeks.

5.3.1. Prepare the mouse for oral gavage by pinching the skin of the back and pinning it backwards so that the head and limbs of the mouse are immobilized.

5.3.2. Insert the gavage probe down the back of the throat until the probe reaches the esophagus. Make sure that the probe is not inserted too far, as the lungs may perforate, causing death.

5.4. Make a MK-8669 stock solution in ethanol at 25 mg/mL. Dilute it in a vehicle containing 5.2% Tween 80 and 5.2% PEG400 in sterile water for IP injections at 10 mg/kg for 5 days every other week, for a total treatment duration of 4 weeks.

NOTE: The volume injected into mice should be 50-120 □l, depending on the animal's weight.

5.5. Use seven to eight mice per group to ensure sufficient statistical power for detecting treatment differences[40,41].

5.6. Assess body weight and general condition of the mice in therapy daily. Withhold administration of drugs if an animal's weight drops 20% or more from its initial weight.

5.7. Assess the tumor size weekly using ultrasound scanning. Make sure that the individual performing monitoring of the tumor growth is blinded to the treatment to ensure unbiased scoring of responses.

NOTE: Smaller laboratories may employ two different people to administer treatment and ultrasound monitoring.

REPRESENTATIVE RESULTS:

Tissue from resected ovarian tumors at the time of debulking surgeries were collected in accordance with IRB guidance and used for 1) genomic characterization and 2) engraftment in immunocompromised mice (**Figure 1**). Mate-pair sequencing[36,37] was used to identify structural alterations in DNA including losses, gains, and amplifications. A representative genome plot illustrating a landscape of genomic changes in one tumor (designated as OC101) is shown in **Figure 2**. Typical for high grade serous subtype tumors, multiple gains (blue lines) and deletions (red lines) were found, indicating high levels of genomic instability, as well as chromosomal losses and gains, indicative of aneuploidy, were observed. Subsequent analyses revealed a few DNA alterations that were potentially targetable with clinically relevant drugs. The top-ranked alteration for therapeutic intervention in the OC101 tumor was an amplification at chromosome 17 involving ERBB2 (**Figure 2, Figure 3A**). ERBB2 is a gene that codes for the HER2 receptor, which is known to (upon dimerization with EGFR, HER3, or HER4) activate RAS/ERK and PI3K/AKT signaling pathways and promote cell growth, cell migration, and invasion. HER2 inhibitors (such as monoclonal antibodies pertuzumab and trastuzumab) are effective in treating breast cancer patients when tumors overexpress the HER2 protein. Anti-HER2 therapy for ovarian cancer, however, is not FDA approved.

Comparison of the genomic profile of a donor patient's tumor (**Figure 1**) to that of a corresponding PDX model (not shown) revealed a striking similarity, consistent with all previous studies reporting the molecular closeness of original tumors to their PDX derivatives.

To validate MPseq results on the DNA level, several sets of specific primers were designed for the edges of amplified region containing the ERBB2 gene, and PCR was carried out using DNA isolated from the original tumor as well as from a tumor propagated for several generations in the mice. A representative gel image of amplified products using two different sets of primers is shown in **Figure 3B**. No band was detected when normal pooled genomic DNA (designated as C), that did not contain amplification of the ERBB locus, was amplified. Purification of products from the gel and Sanger sequencing (not shown) further confirmed the alteration predicted by MPseq. Further validation was conducted by examining the expression of HER2 protein in the corresponding PDX tumor using immunoblotting. The analysis revealed a high level of HER2 protein (result not shown), consistent with observed amplification of the ERBB2 gene.

In the DNA of a different ovarian tumor (designated T14) numerous regional gains were observed. Those included AKT2 and RICTOR genes (**Figure 3C**). Both were of great interest from a therapeutic perspective as inhibitors of AKT2 and mTOR, which RICTOR associates with, are available and currently in clinical trials. Since there were no mate pair reads spanning the vicinity of either gene, simple PCR validation of the gain as detected by MPseq was not possible. The expression level of corresponding proteins were therefore tested by immunoblotting. High levels of AKT and RICTOR were observed (**Figure 3D**), suggesting that treatment with targeted drugs is warranted.

To test the sensitivity of this tumor to inhibitors of AKT and mTOR, PDX mice with intraperitoneally implanted T14 tumor were expanded and randomized to receive only chemotherapy (carboplatin/paclitaxel) or a combination of chemotherapy with pan-AKT inhibitor MK-2206 or mTOR inhibitor MK-8669. Chemotherapy was given to mice in the combination arm for 2 weeks prior to the addition of the targeted therapy (**Figure 4**). Ultrasound measurements were taken weekly to monitor tumor regression/growth.

Each treatment arm contained no less than seven mice. This number was sufficient to observe differences in responses between the groups while keeping costs of the study at a considerably lower mark. Fewer mice (three to four) can be used in the control untreated group, as individual variations in tumor growth rate are negligible and growth is normalized to a tumor size at which treatment in other arms begins.

No difference was observed between chemo-treated and untreated groups in the first 3 weeks of observation (not shown). A significant reduction of tumor burden (58% median) was observed in the chemotherapy treated group by the end of week 6. An extra benefit over chemotherapy alone was observed in groups which received a combination of chemotherapy with targeted therapies. The difference became evident at weeks 4 and 3 for MK-8669 (**Figure 4A**) and MK-2206 (**Figure 4B**) respectively.

Animals were euthanized and tumor tissue was collected for molecular analyses of treatment response at the end of the treatment trial at week 7. For that purpose, the amounts of total and phosphorylated S6 kinase (**Figure 5A,B**), AKT and mTOR (**Figure 5C,D**) were determined using immunoblotting. Ribosomal protein S6 kinase is a downstream messenger of the AKT-mTOR pathway, known to be upregulated and phosphorylated upon stimulation of the AKT-mTOR axis by growth factors to promote cell survival and growth. Comparison of these protein levels in untreated or treated with chemotherapy PDX tumors to those in mice that received AKT or mTOR inhibitors showed a marked decrease in the latter two (**Figure 5**), indicating effectiveness of the targeted therapy on the molecular level. Adjustments to the treatment regiment, as far as application timing for the combined drugs and therapy duration, should be made and tested to achieve better responses.

FIGURE AND TABLE LEGENDS:

Figure 1: Schematic of the strategy for genomically guided therapy testing using PDX models for serous ovarian carcinoma. H&E staining of an ovarian tumor is shown (top).

Figure 2: Genomic characterization of ovarian tumors using MPseq. Genome plot showing the landscape of structural alterations and copy number changes as detected by MPseq. The x-axis spans the length of the chromosome, with chromosome position number shown. Each chromosome is indicated on the right and left y-axes. The height of horizontal traces for each chromosome indicates the number of reads detected for 30k base-pair windows. DNA copy numbers are indicated by color, with grey representing the normal 2N copy state, red

corresponding to deletions, and blue corresponding to gains. Connecting black lines correspond to chromosomal rearrangements. Alterations at ERBB2 locus are depicted.

Figure 3: **Selection of targetable alterations and their validation**. **(A**) A close-up segment of the genome plot shown in **Figure 1,** illustrating an amplification of the ERBB2 gene on chromosome 17 (blue). Chromosome numbers are as indicated. (**B)** Validation analysis of breakpoints at ERBB2 locus as identified by MPseq using PCR amplification. C is a pooled genomic DNA control, OC101 is DNA from patient tumor, and M is a DNA ladder. (**C)** A close-up of segments of the genome plot for another ovarian tumor showing gains (blue line) at the AKT locus (top) and at the RICTOR gene (bottom). Chromosomes are as indicated. (**D)** Validation analysis of expression of proteins of AKT/mTOR pathway by immunoblotting using tumor tissue from PDX (T14), genomic alterations for which are depicted in (C). 30 ug of total protein and specific antibodies to AKT, RICTOR, and p-mTOR were used. MAPK served as a loading control. Pos con = an independent tumor used as a positive control.

Figure 4: The comparison of responses to chemotherapy alone and combined with targeted therapy in tumor harboring gains at AKT2 and RICTOR genes with corresponding drugs. Treatment responses to a combination of chemotherapy and anti-mTOR drug MK-8669 (**A**) or inhibitor of pan-AKT MK2206 (**B**) versus chemotherapy alone. The time of administration for each treatment and duration are shown by the arrows. Volumes are expressed as percent of initial volume at the start of the treatment as mean ± SD. Chemo = chemotherapy.

Figure 5: Comparison of molecular changes elicited by each treatment as determined by immunoblotting analysis. (A) Levels of S6 and phospho-S6, the downstream effector of AKT-mTOR pathway are shown. 30 ug of total protein and specific antibody to S6 and p-S6 were used. GAPDH was used as a loading control. Quantification of protein levels normalized to GAPDH level is shown in (**B). (C)** Levels of mTOR, p-mTOR, AKT and p-AKT as detected by immunoblotting. GAPDH was used as a loading control. **D.** Quantification of protein levels normalized to GAPDH level. NT = not treated, chemo = chemotherapy.

Table 1: Primers used for the validation of the OC101 chromosome 17 alteration.

Table 2: PCR setup to validate a junction.

Table 3: Cycling conditions for PCR to validate a junction.

DISCUSSION:

This paper describes the approach and protocols used to conduct a “clinical trial” in PDX models, which takes advantage of molecular characteristics of a tumor as obtained by genomic profiling to determine the best drug choice for further testing. Multiple sequencing platforms are currently used for genomic characterization of primary tumors including whole genome sequencing, RNAseq, and customized gene panels. For high grade serous ovarian carcinoma, MPseq to identify structural alterations, DNA rearrangements, and copy number changes is

particularly useful because of the high degree of genomic instability observed in this type of tumor. The second advantage of the MPseq platform is that it covers the entire genome and costs significantly less than other comprehensive sequencing technologies. MPseq, however, is not suitable for point mutation detection, as base coverage is not sufficient and reaches only 8-10x. One limitation of using MPseq alone for genomic characterization of a tumor is the presence of complex clustered chromosomal rearrangements, analysis of which does not predict the expression of impacted genes of interest. A junction detected by MPseq predicted to create a putative fusion gene validated in the DNA by PCR may not be expressed because of a frameshift or small deletions and insertions in the promoter region. Similarly, chromosomal gains and amplifications for potential therapeutic targets should be carefully assessed and validated on the RNA or protein level to ensure expression of the gene of interest.

Although, the molecular makeup of the tumor is largely preserved after propagation in mice for several generations, changes in expression levels of key genes may occur over time either reflecting tumor evolution, clonal selection, or adaptive response to murine environment. Thus, validation of an alteration intended for therapeutic intervention in both original donor tumor and PDX tumor is critical. For tumors isolated from PDX models, both RNA and protein can be used to interrogate the expression level, as the material is abundant. Either can be chosen to cross-check expression in the original tumor, depending on the availability and type of stored tissue and availability of antibody for the corresponding protein detection.

The PDX model is specifically invaluable in testing combination therapies, as the *in vivo* setting allows the monitoring of adverse effects as well as dosage or duration adjustments in the treatment regimen. The choice between orthotopic and subcutaneous engraftment can be made depending on the specific questions addressed in the study. However, it is important to keep in mind that the sensitivity of xenografted tumors to therapeutics may be modulated by the site of implantation[42]. On the other hand, no evidence has yet been reported on the discovery of drugs showing therapeutic responses in orthotopic models but no response in subcutaneously implanted PDXs[9].

ACKNOWLEDGEMENTS:
The work was supported by Mr. and Mrs. Neil E. Eckles' gift to the Mayo Clinic Center for Individualized Medicine (CIM).

CONFLICT OF INTEREST:
The authors declare that they have no conflict of interest.

REFERENCES:
1. Tentler, J. J., et al. Patient-derived tumour xenografts as models for oncology drug development. *Nature Reviews Clinical Oncology.* **9,** 338-350 (2012).
2. Marangoni, E. et al. A new model of patient tumor-derived breast cancer xenografts for preclinical assays. *Clinical Cancer Research.* **13**, 3989-3998 (2007).

3. Zhang, X. et al. A renewable tissue resource of phenotypically stable, biologically and ethnically diverse, patient-derived human breast cancer xenograft models. *Cancer Research*. **73**, 4885–4897 (2013).
4. Hidalgo, M. et al. Patient-derived xenograft models: an emerging platform for translational cancer research. *Cancer Discovery*. **4**, 998–1013 (2014).
5. Weroha, S. J. et al., Tumorgrafts as in vivo surrogates for women with ovarian cancer. *Clinical Cancer Research.* **20**, 1288-1297 (2014).
6. Rubio-Viqueira, B. et al. Optimizing the development of targeted agents in pancreatic cancer: tumor fine-needle aspiration biopsy as a platform for novel prospective ex vivo drug sensitivity assays. *Molecular Cancer Therapeutics.* **6**, 1079-1088 (2007).
7. Rubio-Viqueira, B., Hidalgo, M. Direct in vivo xenograft tumor model for predicting chemotherapeutic drug response in cancer patients. *Clinical Pharmacology and Therapeutics.* **85**, 217–221 (2009).
8. Ricci, F. et al. Patient-derived ovarian tumor xenografts recapitulate human clinicopathology and genetic alterations. *Cancer Research.* **74,** 6980-6990 (2014).
9. Fleming, J. M., Miller, T. C., Meyer, M. J., Ginsburg, E., Vonderhaar, B. K. Local regulation of human breast xenograft models. *Journal of Ccellular Physiology.* **224**, 795–806 (2010).
10. Hoffman, R. M. Patient-derived orthotopic xenografts: better mimic of metastasis than subcutaneous xenografts. *Nature Reviews Cancer.* **15**, 451-452 (2015).
11. Jung, J., Seol, H. S., Chang, S. The Generation and Application of Patient-Derived Xenograft Model for Cancer Research. *Cancer Research and Treatment.* **50,** 1-10 (2018).
12. Sivanand, S. et al. A validated tumorgraft model reveals activity of dovitinib against renal cell carcinoma. *Science Translational Medicine.* **4,** 137-152 (2012).
13. Pavía-Jiménez, A., Tcheuyap, V. T., Brugarolas, J. Establishing a human renal cell carcinoma tumorgraft platform for preclinical drug testing. *Nature Protocols.* **9**, 1848-1859 (2014).
14. Fridman, R., Benton, G., Aranoutova, I., Kleinman, H. K., Bonfil, R. D. Increased initiation and growth of tumor cell lines, cancer stem cells and biopsy material in mice using basement membrane matrix protein (Cultrex or Matrigel) co-injection. *Nature Protocols.* **7**, 1138-1144 (2012).
15. Cutz, J. C. et al. Establishment in severe combined immunodeficiency mice of subrenal capsule xenografts and transplantable tumor lines from a variety of primary human lung cancers: potential models for studying tumor progression-related changes. *Clinical Cancer Research.* **12**, 4043–4054 (2006).
16. Siolas, D., Hannon, G. J. Patient-derived tumor xenografts: transforming clinical samples into mouse models. *Cancer Research.* **73**, 5315–5319 (2013).
17. Butler, K. A. et al. Prevention of Human Lymphoproliferative Tumor Formation in Ovarian Cancer Patient-Derived Xenografts. *Neoplasia.* **19**, 628-636 (2017).
18. Cao, X. et al. Defective lymphoid development in mice lacking expression of the common cytokine receptor gamma chain. *Immunity.* **2**, 223–238 (1995).
19. Dobbin, Z. C. et al. Using heterogeneity of the patient-derived xenograft model to identify the chemoresistant population in ovarian cancer. *Oncotarget.* **5**, 8750–8764 (2014).
20. Choi, Y. Y. et al. Establishment and characterisation of patient-derived xenografts as paraclinical models for gastric cancer. Scientific Reports. **6**, 22172 (2016)

21. Malaney, P., Nicosia, S. V., Davé, V. One mouse, one patient paradigm: New avatars of personalized cancer therapy. *Cancer Letters.* **344**, 1-12 (2014).
22. Rosfjord, E., Lucas, J., Li, G., Gerber, H. P. Advances in patient-derived tumor xenografts: from target identification to predicting clinical response rates in oncology. *Biochemical Pharmacology.* **91**, 135-43 (2014).
23. Braekeveldt, N., Bexell, D. Patient-derived xenografts as preclinical neuroblastoma models. *Cell and Tissue Research.* **372**, 233-243 (2018).
24. Perez-Soler, R. et al. Response and determinants of sensitivity to paclitaxel in human non-small cell lung cancer tumors heterotransplanted in nude mice. *Clinical Cancer Research.* **6,** 4932–4938 (2000).
25. Fichtner, I. *et al* Anticancer drug response and expression of molecular markers in early-passage xenotransplanted colon carcinomas. *European Journal of Cancer* **40,** 298–307 (2004).
26. Gao, H. et al. High-throughput screening using patient-derived tumor xenografts to predict clinical trial drug response. *Nature Medicine.* **21**, 1318-25 (2015).
27. Izumchenko, E. et al. Patient-derived xenografts effectively capture responses to oncology therapy in a heterogeneous cohort of patients with solid tumors. *Annals of Oncology.* **28**, 2595-2605 (2017).
28. Bertotti, A. et al. A molecularly annotated platform of patient-derived xenografts ("xenopatients") identifies HER2 as an effective therapeutic target in cetuximab-resistant colorectal cancer**.** *Cancer Discovery.* **1**, 508-23 (2011).
29. Mengelbier, L. H. et al. Intratumoral genome diversity parallels progression and predicts outcome in pediatric cancer. *Nature Communications.* **27**, 6125 (2015).
30. McGranahan, N., Swanton, C. Clonal Heterogeneity and Tumor Evolution: Past, Present, and the Future. *Cell.* **168**, 613-628 (2017).
31. Marusyk, A. et al. Non-cell-autonomous driving of tumour growth supports sub-clonal heterogeneity. *Nature.* **514**, 54–8 (2014).
32. Braekeveldt, N. et al. Neuroblastoma patient-derived orthotopic xenografts reflect the microenvironmental hallmarks of aggressive patient tumours. *Cancer Letters.* **375**, 384-389 (2016).
33. DeRose, Y. S. et al. Tumor grafts derived from women with breast cancer authentically reflect tumor pathology, growth, metastasis and disease outcomes. *Nature Medicine.* **17**, 1514-1520(2011).
34. Das Thakur, M. et al. Modelling vemurafenib resistance in melanoma reveals a strategy to forestall drug resistance. *Nature.* **494**, 251-255 (2013).
35. Girotti, M. R. et al. Application of Sequencing, Liquid Biopsies, and Patient-Derived Xenografts for Personalized Medicine in Melanoma. *Cancer Discovery.* **6**, 286-299 (2016).
36. Murphy, S. J. et al. Mate pair sequencing of whole-genome-amplified DNA following laser capture microdissection of prostate cancer. *DNA Research.* **19**, 395-406 (2012).
37. Smadbeck, J. B. et al. Copy number variant analysis using genome-wide mate-pair sequencing. *Genes Chromosomes and Cancer.* **57**, 459-470 (2018).
38. Paster, E. V., Villines, K. A., Hickman, D. L. Endpoints for mouse abdominal tumor models: refinement of current criteria. *Comparative Medicine.* **59**, 234–241 (2009).
39. Schneider, C. A., Rasband, W. S., Eliceiri, K. W. NIH Image to ImageJ: 25 years of image analysis. *Nature Methods.* **9**, 671–675 (2012).

40. Heitjan, D. F., Manni, A., Santen, R. J. Statistical analysis of in vivo tumor growth experiments. *Cancer Research.* **53**, 6042–6050 (1993).
41. Vargas, R. et al. Case study: patient-derived clear cell adenocarcinoma xenograft model longitudinally predicts treatment response. *NPJ Precision Oncology.* **2**, 14 (2018).
42. Fidler, I. J. et al. Modulation of tumor cell response to chemotherapy by the organ environment. *Cancer and Metastasis Reviews.* **13,** 209-222 (1994).

Figure 1

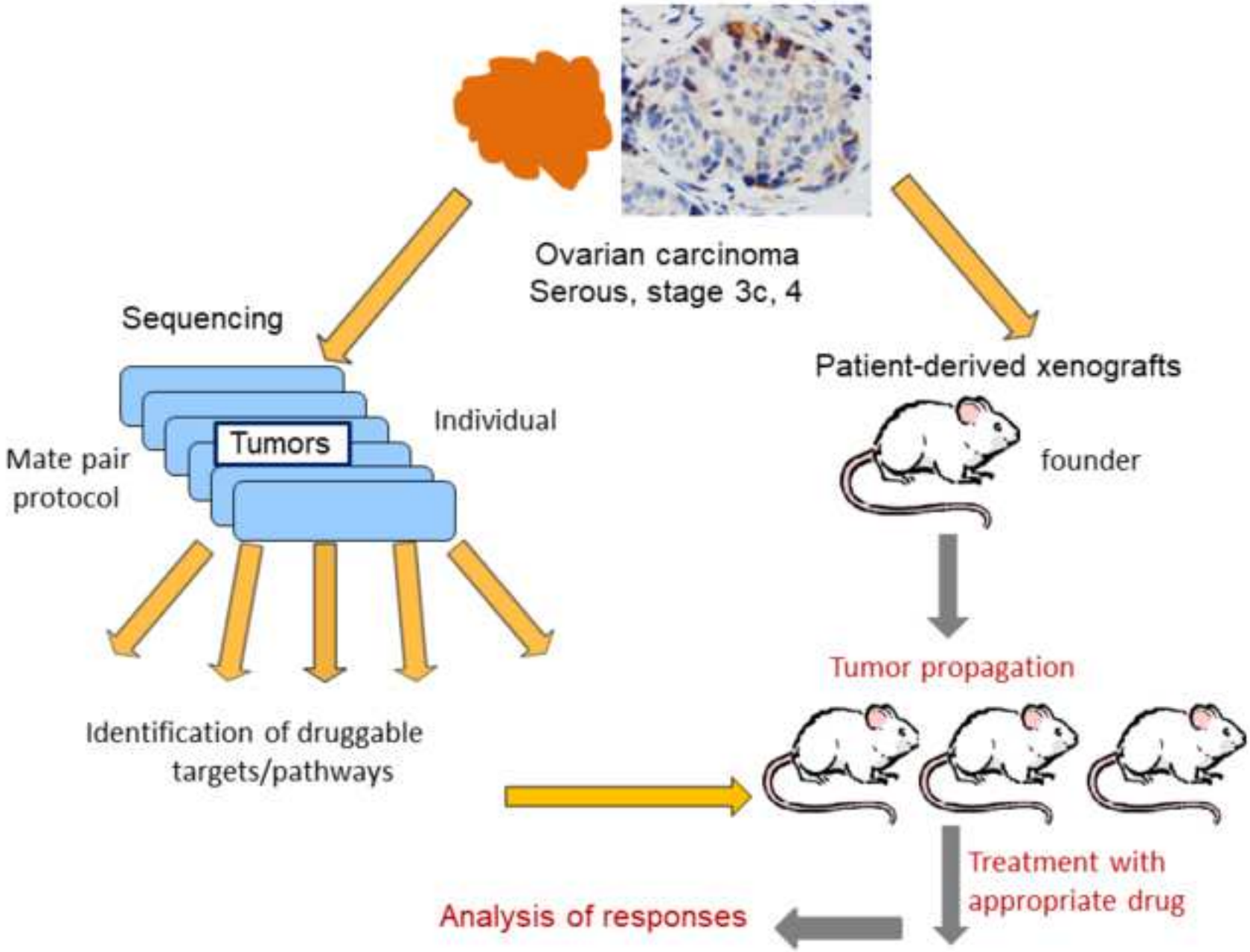

Figure 2

Click here to access/download;Figure;Figure 2.tif

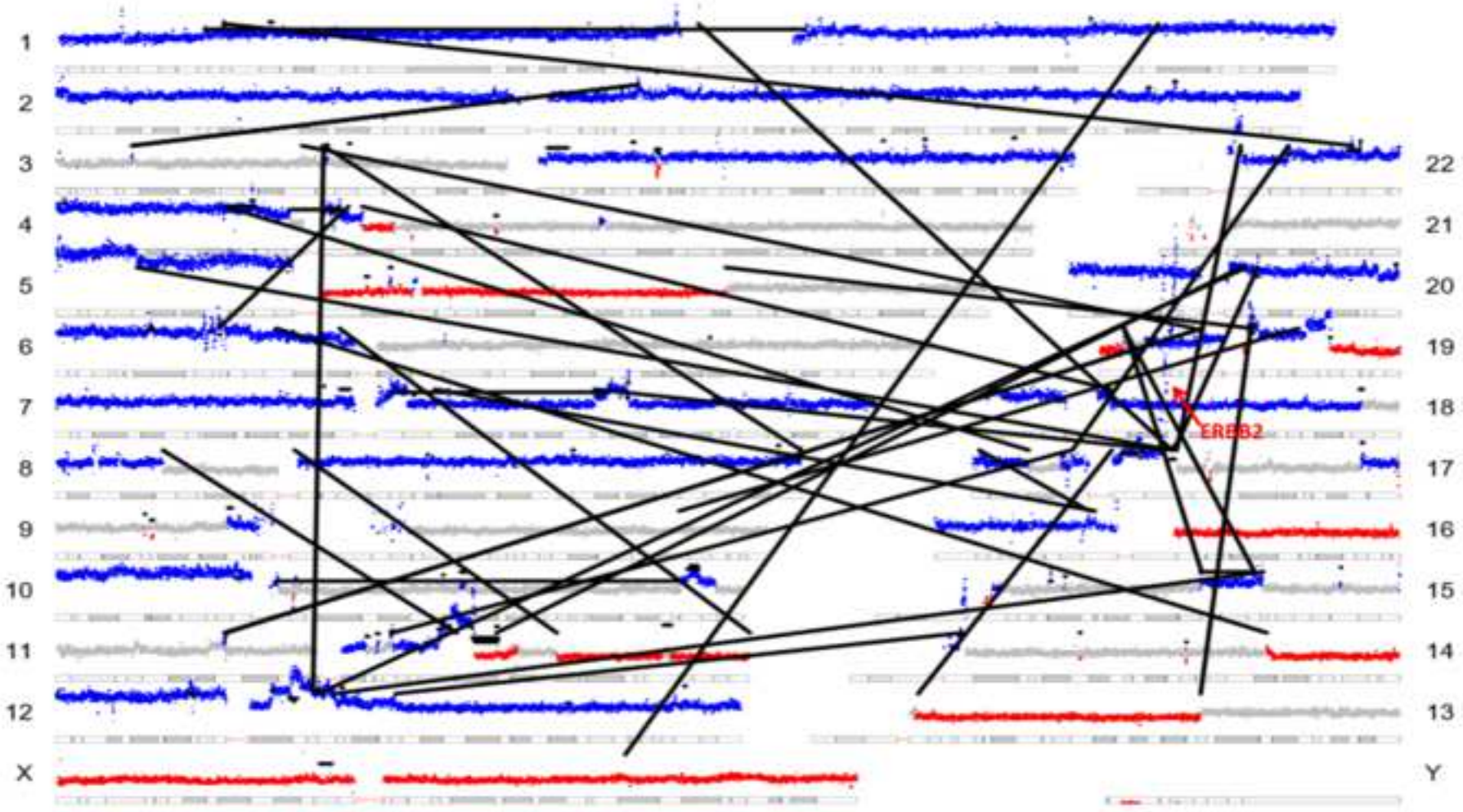

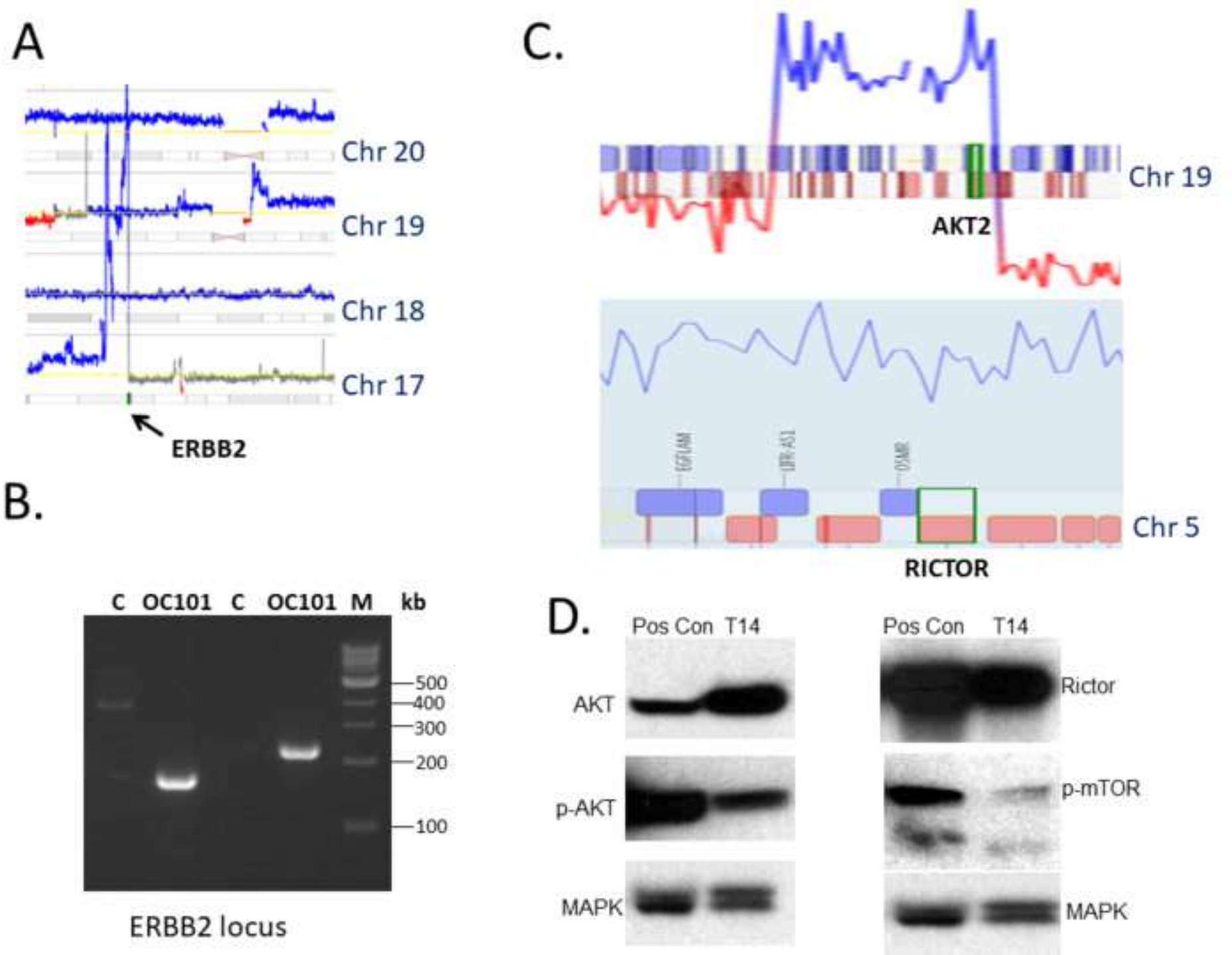

Figure 4

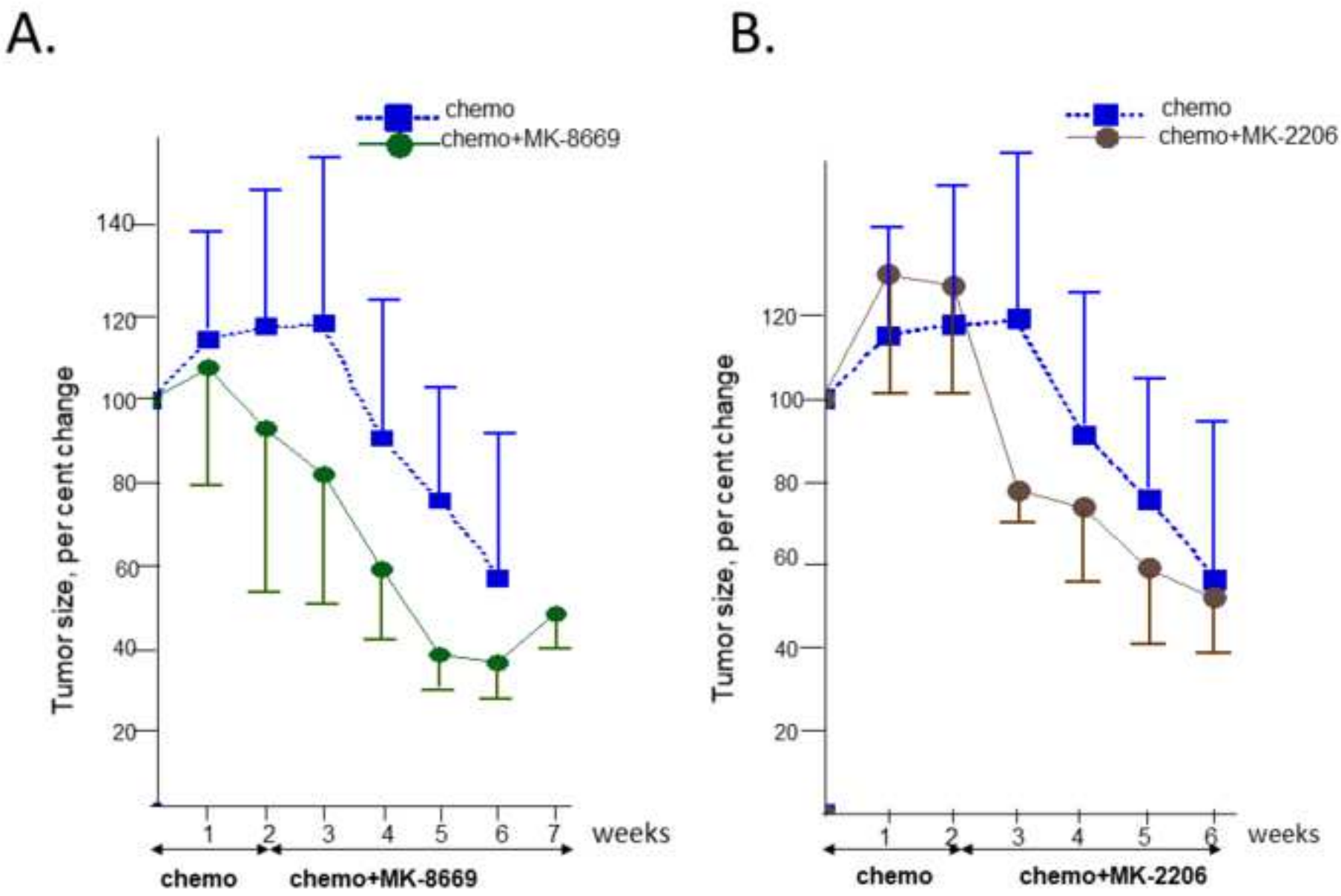

Figure 5

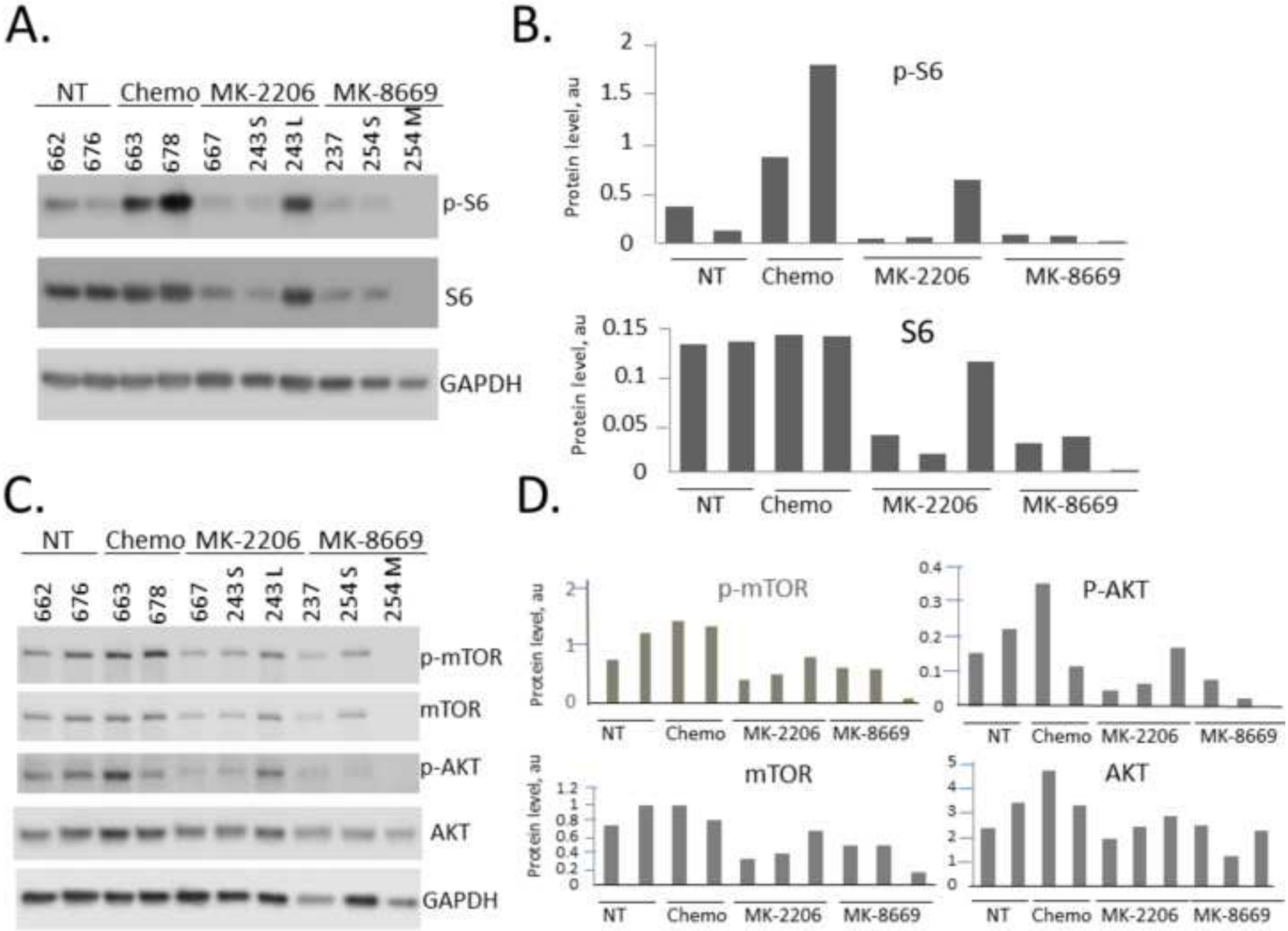

Table 1. Primers used for the validation of the OC101/17 alteration

Primer Name	Sequence	Primer Mix	Primers combined
OC101 17a-1	CTGGTCCTGGGAAATAGACACTAGATAAAT	1	OC101 F1 and R1
OC101 17a-1	GCTCAAGACAGTAACACCTAGTAGTTGATT	2	OC101 F1 and R2
OC101 17b-1	GGATTACGGGAACGTGCTACCTTG	3	OC101 F2 and R1
OC101 17b-1	AATGCCCTAGCAGTTCTATCCCCACTG	4	OC101 F2 and R2

Table 2. Setup for PCR to validate a junction.

Reagent	Quantity to add for 1 reaction (µL)	Quantity to add for 4 reactions (µL). [Multiply by 4.3 to make enough for each primer mix (4)]
Nuclease-free water	20.45	89.94
10x buffer (Easy A)	2.5	10.75
dNTPs 10 mM	0.5	2.15
Template DNA (concentration >10 ng/µL)	0.3	1.29
Taq Polymerase	0.25	1.08

Table 3.Cycling conditions for PCR to validate a junction.

Temp (C)	Time	
94	5 min	
94	40 sec	35 cycles
59	40 sec	
72	2 min	
72	5 min	
4	Hold	

Table of Materials

Click here to access/download;Table of Materials;Materials table edited.xlsx

Name of Material/ Equipment	Company
3M Vetbond	3M, Co.
anti-AKT antibody	Cell Signaling Technologies
Anti-GAPDH antibody(G-9)	Santa Cruz Biotechnology
Anti-MAPK antibody	Cell Signaling Technologies
Anti-phospho-AKT antibody	Cell Signaling Technologies
Anti-mTOR antibody	Cell Signaling Technologies
Anti-Phospho-mTOR antibody	Cell Signaling Technologies
Anti-Phospho-S6 antibody	Cell Signaling Technologies
Anti-Rictor antibody	Cell Signaling Technologies
Anti-S6 antibody	Cell Signaling Technologies
Captisol	ChemScene
Carboplatin	NOVAPLUS
DMEM	Mediatech
Easy-A Hi-Fi PCR Cloning Enzyme	Agilent
Lubricant	Cardinal Healthcare
Matrigel	Corning
McCoy's media	Mediatech
MK-2206	ApexBio
MK-8669	ARIAD Pharmaceuticals
Nair Sensitive Skin	Church & Dwight
NOD/SCID mice	Charles River

Paclitaxel	NOVAPLUS
PEG400	Millipore Sigma
Perjeta	Genetech
Rituximab	Genetech
RPMI1640	Mediatech
SCID mice	Harlan Laboratories
SLAx 13-6MHz linear transducer	FUJIFILM SonoSite
SonoSite S-series Ultrasound machine	FUJIFILM SonoSite
Tween 80	Millipore Sigma

Catalog Number	Comments/Description
1469SB	
9272	
sc-365062	
9926	
9271	
2972	
2971	
4858	
2114	
2217	
cs-0731	
61703-360-18	
10-013-CV	
600404-51	
82-280	
356234	
10-050-CV	
A3010	
AP23573	
Nair™ Hair Remover Shower Power™ Sensitive	
NOD.CB17-*Prkdcscid* /NCrCrl	

55390-304-05

88440-250ML-F

Pertuzumab

Rituxan

10-040-CV

C.B.-17/IcrHsd-*Prkdc*^{scid} *Lyst*^{bg}

HFL38xp

SonoSite SII

P4780-100ML

jove JOURNAL OF VISUALIZED EXPERIMENTS
1 Alewife Center #200
Cambridge, MA 02140
tel. 617.945.9051
www.jove.com

ARTICLE AND VIDEO LICENSE AGREEMENT

Title of Article:	Integrated approach using tumor genomic analyses in conjunction with patient-derived xenografts for testing targeted therapies in cancer\
Author(s):	Lin Yang, Faye R. Harris, Piyan Zhang, George Vasmatzis and Irina V. Kovtun

Item 1: The Author elects to have the Materials be made available (as described at http://www.jove.com/publish) via:

☑ Standard Access ☐ Open Access

Item 2: Please select one of the following items:

☑ The Author is **NOT** a United States government employee.

☐ The Author is a United States government employee and the Materials were prepared in the course of his or her duties as a United States government employee.

☐ The Author is a United States government employee but the Materials were NOT prepared in the course of his or her duties as a United States government employee.

ARTICLE AND VIDEO LICENSE AGREEMENT

1. **Defined Terms.** As used in this Article and Video License Agreement, the following terms shall have the following meanings: "**Agreement**" means this Article and Video License Agreement; "**Article**" means the article specified on the last page of this Agreement, including any associated materials such as texts, figures, tables, artwork, abstracts, or summaries contained therein; "**Author**" means the author who is a signatory to this Agreement; "**Collective Work**" means a work, such as a periodical issue, anthology or encyclopedia, in which the Materials in their entirety in unmodified form, along with a number of other contributions, constituting separate and independent works in themselves, are assembled into a collective whole; "**CRC License**" means the Creative Commons Attribution-Non Commercial-No Derivs 3.0 Unported Agreement, the terms and conditions of which can be found at: http://creativecommons.org/licenses/by-nc-nd/3.0/legalcode; "**Derivative Work**" means a work based upon the Materials or upon the Materials and other pre-existing works, such as a translation, musical arrangement, dramatization, fictionalization, motion picture version, sound recording, art reproduction, abridgment, condensation, or any other form in which the Materials may be recast, transformed, or adapted; "**Institution**" means the institution, listed on the last page of this Agreement, by which the Author was employed at the time of the creation of the Materials; "**JoVE**" means MyJove Corporation, a Massachusetts corporation and the publisher of The Journal of Visualized Experiments; "**Materials**" means the Article and / or the Video; "**Parties**" means the Author and JoVE; "**Video**" means any video(s) made by the Author, alone or in conjunction with any other parties, or by JoVE or its affiliates or agents, individually or in collaboration with the Author or any other parties, incorporating all or any portion of the Article, and in which the Author may or may not appear.

2. **Background.** The Author, who is the author of the Article, in order to ensure the dissemination and protection of the Article, desires to have the JoVE publish the Article and create and transmit videos based on the Article. In furtherance of such goals, the Parties desire to memorialize in this Agreement the respective rights of each Party in and to the Article and the Video.

3. **Grant of Rights in Article.** In consideration of JoVE agreeing to publish the Article, the Author hereby grants to JoVE, subject to **Sections 4** and **7** below, the exclusive, royalty-free, perpetual (for the full term of copyright in the Article, including any extensions thereto) license (a) to publish, reproduce, distribute, display and store the Article in all forms, formats and media whether now known or hereafter developed (including without limitation in print, digital and electronic form) throughout the world, (b) to translate the Article into other languages, create adaptations, summaries or extracts of the Article or other Derivative Works (including, without limitation, the Video) or Collective Works based on all or any portion of the Article and exercise all of the rights set forth in (a) above in such translations, adaptations, summaries, extracts, Derivative Works or Collective Works and(c) to license others to do any or all of the above. The foregoing rights may be exercised in all media and formats, whether now known or hereafter devised, and include the right to make such modifications as are technically necessary to exercise the rights in other media and formats. If the "Open Access" box has been checked in **Item 1** above, JoVE and the Author hereby grant to the public all such rights in the Article as provided in, but subject to all limitations and requirements set forth in, the CRC License.

4. **Retention of Rights in Article.** Notwithstanding the exclusive license granted to JoVE in **Section 3** above, the Author shall, with respect to the Article, retain the non-exclusive right to use all or part of the Article for the non-commercial purpose of giving lectures, presentations or teaching classes, and to post a copy of the Article on the Institution's website or the Author's personal website, in each case provided that a link to the Article on the JoVE website is provided and notice of JoVE's copyright in the Article is included. All non-copyright intellectual property rights in and to the Article, such as patent rights, shall remain with the Author.

5. **Grant of Rights in Video – Standard Access.** This **Section 5** applies if the "Standard Access" box has been checked in **Item 1** above or if no box has been checked in **Item 1** above. In consideration of JoVE agreeing to produce, display or otherwise assist with the Video, the Author hereby acknowledges and agrees that, Subject to **Section 7** below, JoVE is and shall be the sole and exclusive owner of all rights of any nature, including, without limitation, all copyrights, in and to the Video. To the extent that, by law, the Author is deemed, now or at any time in the future, to have any rights of any nature in or to the Video, the Author hereby disclaims all such rights and transfers all such rights to JoVE.

6. **Grant of Rights in Video – Open Access.** This **Section 6** applies only if the "Open Access" box has been checked in **Item 1** above. In consideration of JoVE agreeing to produce, display or otherwise assist with the Video, the Author hereby grants to JoVE, subject to **Section 7** below, the exclusive, royalty-free, perpetual (for the full term of copyright in the Article, including any extensions thereto) license (a) to publish, reproduce, distribute, display and store the Video in all forms, formats and media whether now known or hereafter developed (including without limitation in print, digital and electronic form) throughout the world, (b) to translate the Video into other languages, create adaptations, summaries or extracts of the Video or other Derivative Works or Collective Works based on all or any portion of the Video and exercise all of the rights set forth in (a) above in such translations, adaptations, summaries, extracts, Derivative Works or Collective Works and (c) to license others to do any or all of the above. The foregoing rights may be exercised in all media and formats, whether now known or hereafter devised, and include the right to make such modifications as are technically necessary to exercise the rights in other media and formats. For any Video to which this **Section 6** is applicable, JoVE and the Author hereby grant to the public all such rights in the Video as provided in, but subject to all limitations and requirements set forth in, the CRC License.

7. **Government Employees.** If the Author is a United States government employee and the Article was prepared in the course of his or her duties as a United States government employee, as indicated in **Item 2** above, and any of the licenses or grants granted by the Author hereunder exceed the scope of the 17 U.S.C. 403, then the rights granted hereunder shall be limited to the maximum rights permitted under such statute. In such case, all provisions contained herein that are not in conflict with such statute shall remain in full force and effect, and all provisions contained herein that do so conflict shall be deemed to be amended so as to provide to JoVE the maximum rights permissible within such statute.

8. **Protection of the Work.** The Author(s) authorize JoVE to take steps in the Author(s) name and on their behalf if JoVE believes some third party could be infringing or might infringe the copyright of either the Author's Article and/or Video.

9. **Likeness, Privacy, Personality.** The Author hereby grants JoVE the right to use the Author's name, voice, likeness, picture, photograph, image, biography and performance in any way, commercial or otherwise, in connection with the Materials and the sale, promotion and distribution thereof. The Author hereby waives any and all rights he or she may have, relating to his or her appearance in the Video or otherwise relating to the Materials, under all applicable privacy, likeness, personality or similar laws.

10. **Author Warranties.** The Author represents and warrants that the Article is original, that it has not been published, that the copyright interest is owned by the Author (or, if more than one author is listed at the beginning of this Agreement, by such authors collectively) and has not been assigned, licensed, or otherwise transferred to any other party. The Author represents and warrants that the author(s) listed at the top of this Agreement are the only authors of the Materials. If more than one author is listed at the top of this Agreement and if any such author has not entered into a separate Article and Video License Agreement with JoVE relating to the Materials, the Author represents and warrants that the Author has been authorized by each of the other such authors to execute this Agreement on his or her behalf and to bind him or her with respect to the terms of this Agreement as if each of them had been a party hereto as an Author. The Author warrants that the use, reproduction, distribution, public or private performance or display, and/or modification of all or any portion of the Materials does not and will not violate, infringe and/or misappropriate the patent, trademark, intellectual property or other rights of any third party. The Author represents and warrants that it has and will continue to comply with all government, institutional and other regulations, including, without limitation all institutional, laboratory, hospital, ethical, human and animal treatment, privacy, and all other rules, regulations, laws, procedures or guidelines, applicable to the Materials, and that all research involving human and animal subjects has been approved by the Author's relevant institutional review board.

11. **JoVE Discretion.** If the Author requests the assistance of JoVE in producing the Video in the Author's facility, the Author shall ensure that the presence of JoVE employees, agents or independent contractors is in accordance with the relevant regulations of the Author's institution. If more than one author is listed at the beginning of this Agreement, JoVE may, in its sole

jove JOURNAL OF VISUALIZED EXPERIMENTS
1 Alewife Center #200
Cambridge, MA 02140
tel. 617.945.9051
www.jove.com

ARTICLE AND VIDEO LICENSE AGREEMENT

discretion, elect not take any action with respect to the Article until such time as it has received complete, executed Article and Video License Agreements from each such author. JoVE reserves the right, in its absolute and sole discretion and without giving any reason therefore, to accept or decline any work submitted to JoVE. JoVE and its employees, agents and independent contractors shall have full, unfettered access to the facilities of the Author or of the Author's institution as necessary to make the Video, whether actually published or not. JoVE has sole discretion as to the method of making and publishing the Materials, including, without limitation, to all decisions regarding editing, lighting, filming, timing of publication, if any, length, quality, content and the like.

12. **Indemnification.** The Author agrees to indemnify JoVE and/or its successors and assigns from and against any and all claims, costs, and expenses, including attorney's fees, arising out of any breach of any warranty or other representations contained herein. The Author further agrees to indemnify and hold harmless JoVE from and against any and all claims, costs, and expenses, including attorney's fees, resulting from the breach by the Author of any representation or warranty contained herein or from allegations or instances of violation of intellectual property rights, damage to the Author's or the Author's institution's facilities, fraud, libel, defamation, research, equipment, experiments, property damage, personal injury, violations of institutional, laboratory, hospital, ethical, human and animal treatment, privacy or other rules, regulations, laws, procedures or guidelines, liabilities and other losses or damages related in any way to the submission of work to JoVE, making of videos by JoVE, or publication in JoVE or elsewhere by JoVE. The Author shall be responsible for, and shall hold JoVE harmless from, damages caused by lack of sterilization, lack of cleanliness or by contamination due to the making of a video by JoVE its employees, agents or independent contractors. All sterilization, cleanliness or decontamination procedures shall be solely the responsibility of the Author and shall be undertaken at the Author's expense. All indemnifications provided herein shall include JoVE's attorney's fees and costs related to said losses or damages. Such indemnification and holding harmless shall include such losses or damages incurred by, or in connection with, acts or omissions of JoVE, its employees, agents or independent contractors.

13. **Fees.** To cover the cost incurred for publication, JoVE must receive payment before production and publication the Materials. Payment is due in 21 days of invoice. Should the Materials not be published due to an editorial or production decision, these funds will be returned to the Author. Withdrawal by the Author of any submitted Materials after final peer review approval will result in a US$1,200 fee to cover pre-production expenses incurred by JoVE. If payment is not received by the completion of filming, production and publication of the Materials will be suspended until payment is received.

14. **Transfer, Governing Law.** This Agreement may be assigned by JoVE and shall inure to the benefits of any of JoVE's successors and assignees. This Agreement shall be governed and construed by the internal laws of the Commonwealth of Massachusetts without giving effect to any conflict of law provision thereunder. This Agreement may be executed in counterparts, each of which shall be deemed an original, but all of which together shall be deemed to me one and the same agreement. A signed copy of this Agreement delivered by facsimile, e-mail or other means of electronic transmission shall be deemed to have the same legal effect as delivery of an original signed copy of this Agreement.

A signed copy of this document must be sent with all new submissions. Only one Agreement is required per submission.

CORRESPONDING AUTHOR

Name:	Irina V. Kovtun
Department:	Molecular Pharmacology and Experimental Therapeutics
Institution:	Mayo Clinic
Title:	Assistant Professor
Signature:	IK
Date:	11.05.2018

Please submit a **signed** and **dated** copy of this license by one of the following three methods:

1. Upload an electronic version on the JoVE submission site
2. Fax the document to +1.866.381.2236
3. Mail the document to JoVE / Attn: JoVE Editorial / 1 Alewife Center #200 / Cambridge, MA 02140

MAYO CLINIC

To the Editor: February 21, 2019

Dear Dr. Wu,

Thank you for your quick response. Please find below a detailed description specifying how each editorial comment was addressed.

1. The manuscript was proofread, spelling and grammar errors have been corrected.
2. A step-wise description of software usage was included in step # 3
3. A single space between numerical values and their units was added.
4. Greek characters for SI units were put in place.
5. More details were added to Step 3.2.4.
6. Step 3.2.5 has been modified to be a Note to 3.2.4 instead.
7. The table was removed from the manuscript (Line 193) and uploaded separately as Table 3.
8. Steps describing euthanasia or anesthesia now are not highlighted.
9. The details for anesthetization were added.
10. The importance of maintenance of sterile conditions during survival surgery was emphasized.
11. The step specifying that the animal is not left unattended until it has regained sufficient consciousness to maintain sternal recumbency was added.
12. The step specifying that the animal that has undergone surgery is not returned to the company of other animals until fully recovered.
13. Trademark (™) and registered (®) symbols were removed from the Table of Equipment and Materials.

Sincerely,

Irina V. Kovtun, Ph.D

Assistant Professor
Department of Molecular Pharmacology
And Experimental Therapeutics
Mayo Clinic
Rochester

507-538-0920 (lab)
Email: ivkru@yahoo.com

kovtun.irina@mayo.edu